TWEAK/Fn14 signalling promotes cholangiocarcinoma niche formation and progression.

TWEAK/Fn14 signalling promotes cholangiocarcinoma niche formation and progression

Benjamin J. Dwyer[1,2], Edward J. Jarman[3], Jully Gogoi-Tiwari[2], Sofia Ferreira-Gonzalez[1], Luke Boulter,[1,3] Rachel V. Guest,[1,9] Timothy J. Kendall[10], Dominic Kurian[12], Alastair M. Kilpatrick[1], Andrew J. Robson[1], Eoghan O'Duibhir[1], Tak Yung Man[1], Lara Campana[1], Philip J. Starkey Lewis[1], Stephen J. Wigmore[10,11], John K. Olynyk[4,5] Grant A. Ramm[6,7], Janina E.E. Tirnitz-Parker[2,8*], Stuart J. Forbes[1*]

Affiliations:

[1]*Centre for Regenerative Medicine, Scottish Centre for Regenerative Medicine, University of Edinburgh, Edinburgh, UK*

[2]*School of Pharmacy and Biomedical Sciences, Curtin Health Innovation Research Institute, Curtin University, Bentley, WA, Australia*

[3]*MRC Human Genetics Unit, Western General Hospital Campus, Edinburgh, UK*

[4]*Department of Gastroenterology, Fiona Stanley Fremantle Hospital Group, Murdoch, WA, Australia*

[5]*School of Medical and Health Sciences, Edith Cowan University, Joondalup, WA, Australia*

[6]*Faculty of Medicine, University of Queensland, Brisbane, QLD, Australia*

[7]*QIMR Berghofer Medical Research Institute, Brisbane, QLD, Australia*

[8]*Centre for Cell Therapy and Regenerative Medicine, and School of Biomedical Sciences, University of Western Australia, Nedlands, WA, Australia.*

[9]*Department of Clinical Surgery, University of Edinburgh, Edinburgh EH16 4SA*

[10]*University of Edinburgh Centre for Inflammation Research, Queens Medical Research Institute, University of Edinburgh, Edinburgh EH16 4TJ, United Kingdom*

[11]*Department of Surgery, Royal Infirmary of Edinburgh, Edinburgh EH16 4SA, United Kingdom*

[12]*The Roslin Institute & Royal (Dick) School of Veterinary Studies , University of Edinburgh, Easter Bush , Midlothian EH25 9RG , United Kingdom*

*Equal author contribution

Correspondence: Prof. Stuart J. Forbes, Director of Centre for Regenerative Medicine, Little France Drive, University of Edinburgh, Edinburgh bioQuarter, Edinburgh, United Kingdom, EH16 4UU. E-mail: stuart.forbes@ed.ac.uk, Tel: +44(0)1316519510, Fax: +44(0)1316519501.

Keywords: Cholangiocarcinoma, Liver cancer, TWEAK, Fn14, Tumour-associated macrophage, Cancer-associated fibroblast

Electronic word count (Abstract, Main Text, References, Tables, Figure Legends) : 6568 words

Number of figures and tables: 7 figures, 19 supplementary figures, 4 supplementary tables

Author disclosures: S.J.F. is supported by funds from Wellcome Trust, Medical Research Council, UKRMP and Syncona Ltd.

Financial support: This study was supported by grants from the National Health and Medical Research Council of Australia (APP1031330, APP1087125 and APP1061332) and the Alan Morement Memorial Fund (AMMF) charity.

Author contributions: Conceptualisation and design (B.D., E.J., S.F-G., R.V.G., L.B., J.T.P., S.J.F). Data generation (B.D., E.J., S.F-G., T.K., J.G-T., T-Y. M, A.M.K., L.B., R.V.G., A.R., D.K.), Data analysis and interpretation (B.D., J.G-T.,T.K., L.B., R.V.G., L.C., E.O.D., A.M.K., P.S-L., J.T.P., S.J.F.). Manuscript preparation (B.D., J.T.P, S.J.F). Review and editing (B.D., J.T.P., J.K.O., G.A.R., S.J.F). Funding acquisition (J.T.P., J.K.O., G.A.R., S.J.F).

Data availability: Mass spectrometry data was deposited on the MassIVE repository (https://massive.ucsd.edu/ProteoSAFe/static/massive.jsp, accessible at Proteome Exchange (http://www.proteomexchange.org/; Accession:PXD015317). All other data are available upon reasonable request.

ABSTRACT

Background & Aims: Cholangiocarcinoma (CCA) is a cancer of the hepatic bile ducts that is rarely resectable and associated with poor prognosis. New therapeutic strategies are urgently required. Tumour necrosis factor-like weak inducer of apoptosis (TWEAK) is known to signal via its receptor fibroblast growth factor-inducible 14 (Fn14) and induce cholangiocyte and myofibroblast proliferation in liver injury. Its role in CCA remains undefined.

Methods: The expression of TWEAK ligand and Fn14 receptor was assessed immunohistochemically and by bulk RNA and single cell transcriptomics of human liver tissue. Spatiotemporal dynamics of pathway regulation were comprehensively analysed in rat and mouse thioacetamide (TAA)-mediated CCA. Flow cytometry, qPCR and proteomic analyses of CCA cell lines and conditioned medium experiments with primary macrophages were performed to evaluate TWEAK/Fn14 downstream functions. *In vivo* pathway manipulation was assessed via TWEAK overexpression in NICD/AKT-induced CCA or genetic Fn14 knockout during TAA-mediated carcinogenesis.

Results: Our data reveal TWEAK and Fn14 overexpression in multiple human CCA cohorts, and Fn14 upregulation in early TAA-induced carcinogenesis. TWEAK regulated the secretion of factors from CC-SW-1 and SNU-1079 CCA cells, inducing polarisation of pro-inflammatory $CD206^{+}$ macrophages. Pharmacological blocking of the TWEAK downstream target chemokine monocyte chemoattractant protein 1 (MCP-1) significantly reduced CCA xenograft growth, while TWEAK overexpression drove cancer-associated fibroblast proliferation and collagen deposition in the tumour niche. Genetic Fn14 ablation significantly reduced inflammatory, fibrogenic and ductular responses during carcinogenic TAA-mediated injury.

Conclusion: These novel data provide evidence for the action of TWEAK/Fn14 on macrophage recruitment and phenotype, and cancer-associated fibroblast proliferation in CCA. Targeting TWEAK/Fn14 and its downstream signals may provide a means to inhibit CCA niche development and tumour growth.

Lay summary: Cholangiocarcinoma is an aggressive, chemotherapy-resistant liver cancer. Interactions between tumour cells and cells that form a supportive environment for the tumour to grow are a source of this aggressiveness and resistance to chemotherapy. Herein, we describe interactions between tumour cells and their supportive environment via a chemical messenger, TWEAK and its receptor Fn14. TWEAK/Fn14 alters the recruitment and type of immune cells in tumours, increases the growth of cancer-associated fibroblasts in the tumour environment, and is a potential target to reduce tumour formation.

Graphical abstract:

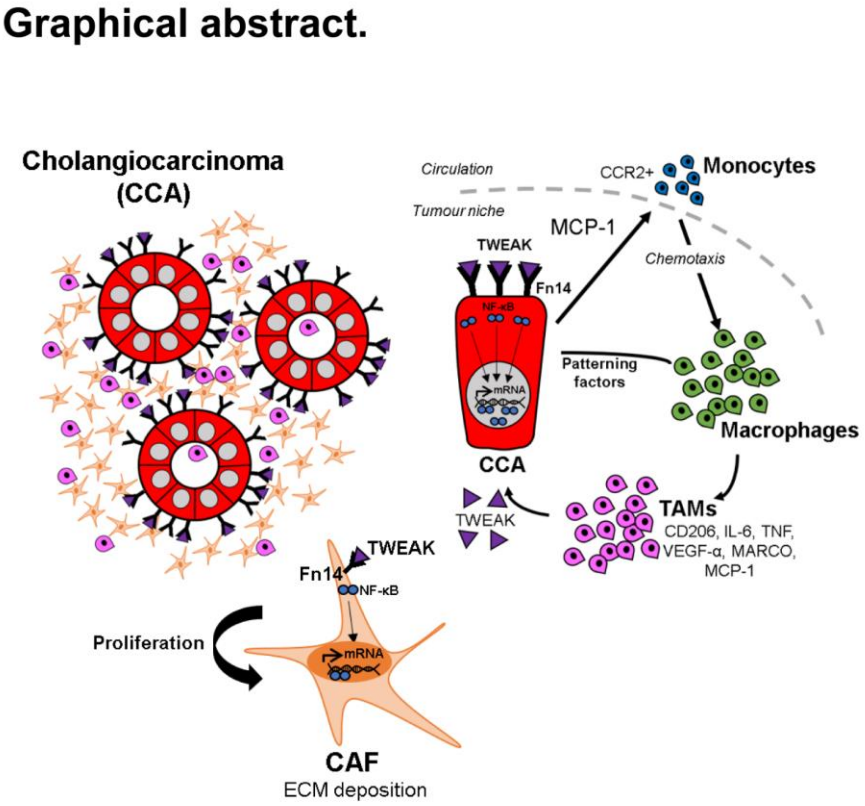

INTRODUCTION

Cholangiocarcinomas (CCA) are aggressive hepatic malignancies, typically adenocarcinomas morphologically resembling hepatobiliary epithelium, expressing cytokeratins (CK) CK7 and CK19 but not CK20 or Hep-Par1[1-3]. CCA occurs at all regions of the biliary tree and is classified according to anatomical location; intrahepatic (iCCA; 20%), peri-hilar (pCCA; 50-60%) or distal (dCCA; 20-30%)[3, 4]. CCA remains clinically challenging due to late-stage presentation, chemotherapy resistance, and high post-surgery recurrence [3]. Consequently, 5-year survival rates remain below 25% [5].

CCA develops a characteristic thick, fibrous stroma composed of α-smooth muscle actin (αSMA)-expressing cancer-associated fibroblasts (CAFs), tumour-associated macrophages (TAMs), neutrophils and vascular endothelial cells [3]. Stromal cells interact with neoplastic ducts via several signals including Wingless-related integration site (Wnt) [6, 7], Notch [8, 9], Platelet-Derived Growth Factor [10, 11], Stromal-Derived Factor-1/C-X-C chemokine receptor type-4 [12, 13] and numerous cytokines, to support growth, evasion of apoptosis and promote metastatic progression via modulation of protein kinase-B (AKT) and extracellular signal-regulated kinase (ERK) pathways [13-15]. $CD14^+/CD16^+$ peripheral blood monocytes are elevated in patients [16], and are recruited to tumour areas, where they differentiate into TAMs [17, 18]. TAM infiltration is correlated with tumour recurrence, metastasis and decreased survival [17, 19]. Fluorescently-tagged bone marrow-derived macrophages comprise the majority of $CD206^+$ TAMs in a rat CCA model, and secrete tumour-feeding Wnt ligands [7]. Ablating TAMs significantly reduces tumour formation, highlighting the importance of macrophage-derived factors in maintaining CCA [7].

The TNF-like weak inducer of apoptosis (TWEAK)/fibroblast growth factor-inducible 14 (Fn14) pathway acts via TWEAK ligand binding to its cognate receptor, Fn14, activating NF-κB/MAPK/PI3K/AKT downstream signalling [20] to regulate proliferation, survival, inflammation and angiogenesis. TWEAK is ubiquitously expressed in adult liver by macrophages, with signalling modulated by dynamic regulation of Fn14 during injury and repair [20, 21]. TWEAK initiates non-hepatocyte-mediated regeneration via canonical NF-κB-induced cholangiocyte proliferation [21, 22] and drives fibrosis-mediating hepatic stellate cell proliferation within the injury niche [23]. TWEAK-expressing macrophages were recently identified as key drivers of fibrosis, controlling $Fn14^{+}$ HSC proliferation in human cirrhotic liver [24]. TWEAK also stimulates proliferation of hepatocellular carcinoma cell lines [25], potentiating a role in liver cancer growth.

We hypothesised that the principal role of TWEAK during chronic liver disease and CCA development may be two-fold: (i) to act as a canonical NF-kB pathway-driven mitogen controlling neoplastic duct and CAF proliferation and (ii) to induce NF-kB-driven chemotaxis-associated signalling during the establishment, maintenance and progression of CCA. We demonstrate that the TWEAK/Fn14 pathway is increasingly expressed during multi-species CCA development, regulating proliferation, migration and polarisation of cells, including macrophages and CAFs in the tumour niche, establishing TWEAK/Fn14 signalling as a novel, therapeutically targetable driver of CCA development.

MATERIALS AND METHODS

Study approval

Animal experiments were approved by the University of Edinburgh animal ethics committee with U.K. Home Office approval (70/7847, 70/8150, P231C5F81) or performed according to the Australian code for the care and use of animals for scientific purposes at Curtin University (AEC_2014_29). Retrospectively collected specimens were obtained from the National Health Service Lothian Scottish Academic Health Sciences Collaboration BioResource and healthy liver from the Edinburgh Medical Research Council Sudden Death Tissue Bank (10/H0716/3). Human blood was collected under ethical approval from the University of Edinburgh (15-HV-013). All human tissue samples were collected with informed consent.

All other methods can be found in the Supplementary Materials and Methods or the Supplementary CTAT Table.

RESULTS

1. TWEAK and Fn14 upregulation in multi-species CCA

We assessed Fn14 expression in archival CCA samples and interrogated publicly available mRNA expression data to ascertain whether the TWEAK/Fn14 pathway was overexpressed in CCA, and to define cell type interactions of ligand and receptor. In a cohort of pathologically confirmed human iCCA cases, Fn14 was highly expressed by malignant epithelia, localising at the surface of these cells. Lower expression was observed in bile ducts in surrounding liver (SL) areas of non-tumour liver tissue, with diffuse staining in hepatocytes. Fn14 was identifiable in endothelial cells within portal triads. Positive stromal cell staining consistent with CAFs was observed in a subset of samples (Figure 1A). Quantification confirmed

increased Fn14 expression in CCA versus non-CCA areas (Figure 1B), corroborated by interrogation of publicly available transcriptomic data. In a scRNA-seq dataset (GSE125449; [26]), *Fn14* was mainly expressed by malignant cells, and subsets of CAFs and hepatic progenitor cells (HPCs). *TWEAK* expression was mainly observed in a subset of TAMs in iCCA (Figure 1C). *Fn14* and *TWEAK* were significantly upregulated in tumour tissue versus non-involved liver in the TCGA-Chol cohort (Supplementary Figure 1A) and in a microarray dataset (GSE26566; [27]: Supplementary Figure 1B).

We then assessed the distribution of Fn14 in $PanCK^+$ tumour epithelia and αSMA^+ CAFs in an iCCA tissue microarray, where 42.50% of tumour cells (n=83 samples containing $PanCK^+$ cells) and 62.64% of CAFs (n=79 samples containing αSMA^+ CAFs) expressed Fn14 (Figure 1D). We observed a greater proportion of $Fn14^+$ CCA cells in well-differentiated (grade 1) versus poorly differentiated (grade 3) iCCAs, but no association between tumour grade and the proportion of $Fn14^+$ CAFs (Figure 1D). No association was observed between TNM stage and proportion of $Fn14^+$ cells (Supplementary Figure 1C), supported by assessment of TCGA-Chol samples with respect to TNM stage (Supplementary Figure 1D).

Since archival human tissue samples represent end-stage CCA, we performed time course analyses to observe the temporal relationship of TWEAK/Fn14 expression to CCA development using rodent models of thioacetamide (TAA)-mediated injury (Figure 2A). Histological examination of Fn14-stained serial sections by a specialist liver histopathologist found that Fn14 was readily identifiable in dysplastic biliary lesions and early CCA (10-18 weeks; Supplementary Figure 2A). Similar to human data, Fn14 was observed at the cell surface of biliary lesions/CCA cells, some endothelial cells and transiently in damaged

hepatocytes (Supplementary figure 2). Fn14 was transiently upregulated in PanCK$^+$ ducts and surrounding damaged hepatocytes at 10 weeks (Figure 2B and Supplementary Figure 2A), which reduced as injury progressed and more PanCK$^+$ cells were detected. As malignancy developed, subsets of PanCK$^+$ cells expressing Fn14 emerged. Fn14 expression continued in CCA epithelia but not in non-malignant ducts (Figure 2B and Supplementary Figure 2B). Biphasic Fn14 expression was mirrored transcriptionally, peaking at 10 and 20 weeks of TAA treatment. *TWEAK* mRNA increased steadily over the time course (Figure 2C). Transcripts of the pro-fibrotic markers collagen type 1α1, transforming growth factor-β1, tissue inhibitors of metalloproteinases (*Timp1, Timp2*) and matrix metalloproteinases (*MMP2, MMP9*) exhibited a comparable biphasic expression (Supplementary Figure 3).

We assessed expression of TWEAK ligand and Fn14 receptor in a transgenic model of CCA induction, where CCA develops during TAA treatment in livers with CK19-inducible Cre-recombinase driven p53-deficiency, but not in mice with at least one functional p53 allele (Figure 2D; [28]). TAA-treated K19-p53$^{f/f}$ mice significantly increased *TWEAK* and *Fn14* mRNA and protein levels during CCA formation, compared to mice without CCA (K19-p53$^{flox/WT}$ and K19-p53$^{WT/WT}$; p53$^{WT/het}$), measured by qPCR (Figure 2E) and Fn14 by western blotting (Figure 2F).

These data associate the transition of normal duct epithelium to iCCA with the upregulation of TWEAK/Fn14 pathway and suggest a potential function during development and maintenance in multi-species CCA.

2. TWEAK/Fn14 modulates NF-κB-regulated cytokine/chemokine secretion in CCA cells

To assess function of TWEAK/Fn14 in CCA epithelia, we studied the effects of recombinant human TWEAK (rhTWEAK) treatment in four well-characterised iCCA cell lines, all expressing cell surface Fn14 (Supplementary Figure 4A). TWEAK stimulation uniformly induced canonical p65 NF-κB phosphorylation, processing of non-canonical NF-κB p100 to p52 in CC-SW-1 and SNU-1079 cells (Figure 3A), and stimulated nuclear translocation of p65 in CCA cells (Figure 3B). Despite consistent rhTWEAK-mediated NF-κB activation in all cell lines, only SNU-1079 and HuH-28 cells displayed a mitogenic response to rhTWEAK (Figure 3C).

NF-κB regulates a variety of pro-inflammatory and pro-fibrogenic responses in liver disease [29]. Since a key element of CCA development is the formation of a stimulatory, pro-tumorigenic niche, we investigated TWEAK-induced gene expression changes in CCA cells. We observed TWEAK-inducible mRNA expression of *MCP-1* (3/4 cell lines), *CX_3CL_1* (3/4 cell lines), *IL-6* (1/4 cell lines), *IL-8* (3/4 cell lines), *M-CSF* (3/4 cell lines) and *GM-CSF* (2/4 cell lines) (Figure 3D). To determine pathway specificity, we assessed TWEAK-inducible gene expression in the presence and absence of inhibitors of canonical or non-canonical NF-κB signalling in CCA versus HCC cells. Generally, TWEAK-induced gene expression was subdued by canonical NF-κB inhibition in CCA lines. *IL-6* was inhibited by both inhibitors, whereas *CX_3CL_1* and *M-CSF* were not affected by either inhibitor in CC-SW-1 cells. Likewise, *CX_3CL_1* expression was not affected by either inhibitor in HuH-28 cells. TWEAK-induced gene expression was not observed in HepG2 HCC cells (Supplementary Figure 4B).

We observed significantly increased TWEAK-induced secretion of MCP-1 (all cell lines), IL-8 (2/4 cell lines) and GM-CSF (all cell lines) into the cell culture medium (Figure 3E). We also

characterised proteins present in conditioned medium from PBS- or TWEAK-treated cells by mass spectrometry. Secreted proteins that were present in both PBS- and TWEAK-treated cell line conditioned medium, or in TWEAK-treated conditioned medium alone, were assessed for protein-protein interactions and 'biological process' gene ontology (GO) enrichment (Supplementary Figures 5-8). Several GO terms associated with pro-tumour microenvironment development were enriched in TWEAK-conditioned medium, including extracellular matrix (ECM) development (ECM organisation), blood vessel development (angiogenesis, blood vessel remodelling/development) and immune modulation (regulation of leukocyte/macrophage chemotaxis, immune system process, immune response) in a cell line-specific manner.

These cell line-specific results classified the investigated $Fn14^{+}$ iCCA lines as TWEAK-high responder (CC-SW-1 and SNU-1079) and TWEAK-low responder cell lines (CC-LP-1 and HuH-28) and provided evidence that TWEAK/Fn14 may play a role in the development of CCA by orchestrating the surrounding niche via localised NF-κB-mediated chemokine/cytokine secretion.

3. TWEAK-induced CCA-derived factors regulate macrophage biology

Tumour-associated macrophages (TAMs) play a critical role in providing pro-proliferative and pro-survival factors in CCA [7]. Since TWEAK induces the secretion of several pro-inflammatory proteins in CCA cells, we investigated whether any of these TWEAK-induced, CCA-derived secreted proteins could affect macrophage phenotypes. To model the effect of TWEAK in CCA-induced patterning of macrophages in the CCA niche, we isolated human peripheral blood monocytes (Supplementary Figure 9A), differentiated these cells into macrophages (HMDMs) and subjected HMDMs to (a) PBS-supplemented basal medium

versus (b) TWEAK-supplemented basal medium, to assess the direct effects of TWEAK in HMDMs; or to (c) conditioned medium of 72 hours PBS-treated CCA cell lines versus (d) conditioned medium of 72 hours TWEAK-treated CCA cell lines, to measure the indirect effects of TWEAK in HMDMs via TWEAK-induced protein secretion in the CCA cell lines.

HMDM differentiation was confirmed by 25F9 expression (Supplementary Figure 9B). Treatment with conditioned medium from TWEAK-stimulated TWEAK-high responder CCA lines (CC-SW-1 and SNU-1079) significantly increased cell surface expression of a TAM-associated marker, CD206, in HMDMs. No significant difference was observed when conditioned medium from TWEAK-low responder CCA lines (CC-LP-1 and HuH-28 cells) was used (Figure 4A), suggesting that TWEAK-induced factors from some CCA cells can induce macrophage polarisation. We also assessed mRNA expression of several cytokines, chemokines, growth factors and receptors. HMDMs expressed 154- to 733-fold less *Fn14* mRNA than CCA/HCC cell lines (Supplementary Figure 9C) and did not modulate gene expression when treated with TWEAK alone (Figure 4B). Few genes were differentially regulated in HMDMs exposed to conditioned medium from the TWEAK-low responder CCA cells (*MMP-2* in TWEAK-conditioned medium from CC-LP-1 cells, and *TWEAK* and *CD163* mRNA in TWEAK-conditioned medium from HuH-28 cells). However, expression of several key transcripts was induced in HMDMs treated with TWEAK-conditioned medium from CC-SW-1 and SNU-1079 cells. *IL-6* was upregulated in TWEAK-conditioned medium from both cell lines (82.6-fold and 105.2-fold), and *TIMP-1* (4.5-fold and 4.3-fold). In CC-SW-1 conditioned medium-patterned cells, we observed additional upregulation of *CD80* (2.8-fold), *M-CSF* (6.2-fold) and *TNF* (3.9-fold). SNU-1079-patterned cells responded with additional upregulation of *MCP-1* (4.0-fold) and vascular endothelial growth factor-alpha (*VEGF-α*; 4.5-fold). We also assessed two surface markers associated with TAMs; triggering receptor expressed on myeloid cells 2 (*TREM-2*) and macrophage receptor with collagenous structure

(*MARCO*). All populations expressed *TREM-2*, and SNU-1079-patterned cells upregulated *MARCO* (18.1-fold; Figure 4B).

4. MCP-1 is upregulated in CCA and affects macrophage accumulation in the tumour niche

MCP-1 was the most abundant TWEAK-inducible protein produced by CCA cell lines (Figure 2). In addition, MCP-1 was upregulated in macrophages by TWEAK-inducible factors produced by CCA cells (Figure 4). We therefore further investigated MCP-1 expression in CCA to link in vitro observations to human disease. In analysis of a scRNA-seq dataset (GSE125449; [26]), *MCP-1* mRNA was expressed by CAFs, and subsets of tumour cells, HPCs and TAMs, while cognate receptor *CCR2* was mainly expressed in TAMs and T cells (Supplementary Figure 10A). We observed increased MCP-1 immunostaining in archival human iCCA in tumour epithelia and widespread expression in stromal cells, compared to a subset of paired non-involved surrounding liver areas (Figure 5A), confirmed by pixel analysis (Figure 5B*).*

Next, we assessed the co-regulation of the TWEAK/Fn14 pathway and MCP-1 expression in CCA epithelia. We stratified PanCK$^+$ epithelial tumour cells into Fn14$^+$ and Fn14$^-$ subsets, assessed the distribution of MCP-1$^+$ cells in iCCA and further assessed these data with respect to tumour grade (Figure 5C). Importantly, MCP-1 expression was proportionally higher in Fn14$^+$ versus Fn14$^-$ iCCA ducts in this cohort (Figure 5D; n=89). When stratified by tumour grade, this distribution was maintained in moderately differentiated grade 2 tumours ($p<0.0001$, n=32;) and poorly differentiated grade 3 tumours ($p=0.0014$, n=44; Figure 5D). This preferential distribution of MCP-1$^+$ cells to Fn14$^+$ tumour epithelia was also observed in our cohort of archival sections of iCCA patients and another commercially available CCA

tissue microarray (Supplementary Figure 10B), suggesting an active TWEAK/Fn14/MCP-1 axis in a significant proportion of CCAs across three independent cohorts.

We further assessed MCP-1 protein expression in two key components of the tumour niche; TAMs ($CD68^+$) and CAFs (αSMA^+). MCP-1 was expressed by 18.26% of $CD68^+$ TAMs and 18.52% of CAFs compared to 27.98% of malignant epithelia in this cohort of tumours (n=88-90; Figure 5E). Having confirmed MCP-1 upregulation in clinical samples, we explored the temporal modulation and functional significance of MCP-1 upregulation during CCA development in rodent models.

In rat CCA, small clusters of MCP-1^+ cells were detected during early tumour development (Figure 6A). MCP-1 was expressed specifically in $PanCK^+$ epithelia in tumour niches containing large areas of accumulated TAMs ($CD68^+$; Figure 6B). *MCP-1* mRNA also exhibited the bi-phasic expression observed for *Fn14*, increasing again after peak *Fn14* expression was observed during tumour formation (Figure 6C). MCP-1 was also expressed by CCA tumour cells in our previously described transgenic TAA CCA model [28] (Figure 6D), suggesting a critical, conserved role for MCP-1 during multi-species CCA development.

To investigate the functional role of MCP-1 in recruiting macrophages to the CCA niche, we performed pharmacological blocking experiments using SNU-1079-generated human CCA cell xenografts (Figure 6E). Mice receiving multiple injections of anti-MCP-1 antibody formed significantly smaller tumours (Figure 6F), with 2.3-fold fewer intra-tumoral $F4/80^+$ macrophages (Figure 6G), and 2.2-fold fewer $CD206^+$ macrophages (Figure 6G), compared to control antibody-treated xenografts. We observed significantly more circulating MCP-1 receptor ($CCR2^+$) monocytes in anti-MCP-1-treated animals (Figure 6H). Although

subcutaneous xenografts do not recapitulate the entire liver microenvironment, they enable modelling of interactions between circulating immune cells and human CCA cells. Thus, these data provide a key functional context of the role of MCP-1 expression in CCA with in vivo evidence that recruitment of tumour-associated macrophages occurs via chemoattraction of $CCR2^+$ monocytes.

5. TWEAK signalling modulation affects tumour formation in vivo

To characterise the effects of TWEAK on CCA tumour development, we used a previously described system of NICD and AKT overexpression in hepatocytes to induce CCA in six weeks (combination referred to as NICD/AKT, [30]). We compared tumours in this model to NICD/AKT tumours overexpressing TWEAK (combination referred to as NICD/AKT+TWEAK). The construct used to overexpress TWEAK also expressed red fluorescent protein (RFP), facilitating concurrent assessment of the localisation of TWEAK-overexpressing cells (Supplementary Figure 11A). Macroscopic white, cyst-like lesions were observed on the surface of NICD/AKT livers (Figure 7A and Supplementary Figure 12A), analogous to previously published observation [30]. TWEAK overexpression produced striking alterations in the appearance of livers, with sizeable bile-containing cysts observed on the surface (Figure 7A, Supplementary Figure 12B).

Microscopic histological characterisations of tumours using blinded assessment by an independent, specialist liver histopathologist revealed features that were consistent with this model [30]; tumours consisted of multifocal nodular lesions, often coalescing, precluding quantification of tumour number. Tumours were variably cystic and micropapillary epithelial neoplasms with cytological epithelial features in keeping with malignancy, with TWEAK overexpression increasing the cystic content of these tumours (Figure 7B, Supplementary

Figure 11B). Formal observer-independent quantification of tumour elements showed that TWEAK overexpression increased the total tumour area and cystic percentage of tumours (Figure 7C). The tumour epithelial area was not altered by TWEAK overexpression (Figure 7C). Accordingly, $CK19^+$ epithelium with active, nuclear localisation of phosphorylated NF-κB p65 in either bile duct or CCA tissue was similar in both conditions (Figure 7D), and most CCA cells were proliferating ($Ki67^+$; Figure 7E), presumably as a result of AKT overexpression [30]. We did not find an association between the tumour cystic grade and the proportion of $Fn14^+$ cells in CCA cells or CAFs in patient tissues (Supplementary Figure 13).

Complementing our xenograft results, we observed increases in innate immune cells with TWEAK overexpression, including $CD11b^+$ monocyte/neutrophils that clustered within the tumour niche in cystic tumour areas (Supplementary Figure 11C), and a 2-fold increase in $CD206^+$ macrophage numbers (Supplementary Figure 11C). In addition, GM-CSF was upregulated in liver and plasma with TWEAK overexpression (Supplementary Figure 11D).

TWEAK overexpression also significantly affected the CAF subcompartment of the CCA niche, previously shown to express $Fn14^+$ in patient iCCAs (Figure 1). We detected a 1.32-fold increase in the αSMA^+ CAF area and the Picrosirius Red-positive collagen area in NICD/AKT+TWEAK tumours (Figure 7F). TWEAK activation of canonical NF-κB signalling, demonstrated by an increased proportion of CAFs expressing nuclear phospho-p65 (Figure 7G), has previously been shown to drive hepatic stellate cell proliferation in chronic liver injury [23]. We observed a 1.53-fold increase in proliferating $Ki67^+/\alpha SMA^+$ CAFs in TWEAK-overexpressing CCAs (Figure 7G).

Having established novel roles of TWEAK in inflammatory and fibrogenic niche development in CCA, critical components of a tumour-permissive environment [31], we assessed TAA-mediated chronic liver disease in homozygous Fn14 knockout mice compared to wildtype Fn14-expressing littermate controls (Supplementary Figure 14A). Following six months of TAA injury, significant macroscopic tumour formation was observed in Fn14 wildtype mice (12/12 animals with one or multiple tumours; 2, <2 mm; 9, 2-5 mm, 1, >5 mm diameter), while 1/9 Fn14 knockout mice displayed an early tumour of less than 2 mm in diameter (Supplementary Figure 14B). Concomitant with tumour inhibition in Fn14 knockout mice, we observed a reduction in $PanCK^+$ cells as well as $F4/80^+$ and $CD206^+$ macrophages (Supplementary Figure 14C, 14D). MCP-1, GM-CSF, IL-6 and KC/Gro remained at steady-state levels in 6-month TAA-treated mice (Supplementary Figure 14E). These data support our hypothesis that TWEAK/Fn14 signalling plays a pivotal role in niche establishment during chronic liver injury, capable of supporting hepatic tumour development.

DISCUSSION

During chronic liver injury, macrophage-produced TWEAK drives proliferation of $Fn14^+$ cholangiocytes to initiate hepatic regeneration [21, 22, 32] and αSMA^+ myofibroblasts, affecting extracellular matrix deposition in damaged liver areas by regulating their cell numbers [23, 24]. Macrophages comprise the majority inflammatory cell infiltrate in the CCA stroma [15-17, 19], providing key signals such as Wnt ligands to induce growth and apoptosis resistance [6, 7], and cytokines including IL-6, TNF and TGF-β1 to promote metastatic progression [15, 17]. We hypothesised that TWEAK/Fn14-induced downstream signalling represents a significant pathway, supporting CCA growth and maintenance.

Through corroboration of transcriptomic data from multiple independent CCA patient cohorts and characterisation of patient samples, we demonstrated upregulation of Fn14 in CCA, on tumour epithelial cells and CAFs, compared to non-involved liver tissue. Significantly, a subset of TWEAK-expressing TAMs localised within the CCA niche, suggesting interplay between ligand-expressing niche and receptor-expressing tumour/niche via TWEAK/Fn14, potentiating therapeutic targeting. We demonstrated that TWEAK/Fn14 pathway elements are progressively upregulated in rodent CCA tissues. Previous studies reported proliferation of biliary epithelial, and HCC cells, in response to TWEAK [21, 22, 25, 32]. We explored the effects of TWEAK in CCA lines, and found TWEAK elicited NF-κB signalling modulations in all investigated CCA cell lines, but not HepG2 HCC cells. However, this signal led to cell line-specific cellular responses, suggesting more complex functions for TWEAK/Fn14 signalling in CCA.

In chronic injury, NF-κB controls the expression of a multitude of chemokines and growth factors that regulate liver inflammation and repair, including MCP-1 [33], while aberrant expression of NF-κB pathway components results in spontaneous liver fibrosis and eventual HCC in genetic mouse models [34-36]. Although TWEAK-responsive NF-κB pathway activation was seen in all CCA cell lines we assessed, we did not observe consistent proliferative effects, as reported in other liver cell types [21, 22, 25]. In response to TWEAK stimulation, CCA cells secreted proinflammatory chemokines and growth factors, suggesting TWEAK can regulate CCA niche development. We further explored the functional role of MCP-1, which drives inflammatory macrophage recruitment to sites of liver injury via its receptor CCR2 [37, 38]. Disrupting MCP-1/CCR2 has proven effective in inhibiting TAM accumulation and tumour development in preclinical HCC models [39, 40]. We observed in vitro TWEAK-inducible MCP-1 expression and detected MCP-1 in tumour cells in multi-species CCA. MCP-1 inhibition reduced SNU-1079 xenograft size, with accumulation of

CCR2^{+} monocytes in peripheral blood and decreased TAMs, providing evidence for an MCP-1-mediated macrophage recruitment to the tumour niche by CCA cells. Further support for this axis having a functional role is provided by our data from TAA-treated Fn14 knockout mice, which displayed significantly reduced macrophages and drastically inhibited or delayed tumorigenesis.

We also report a novel function of TWEAK in the liver in driving the secretion of factors from CCA cells that alter macrophage phenotype. CCA cells actively educated macrophages towards a TAM-like phenotype, expressing a mixture of classically activated and alternative activation markers, as well as upregulating molecules involved in matrix remodelling [18]. In TWEAK-high responsive CCA cell lines (SNU-1079 and CC-SW-1), we observed an increased ability to pattern macrophages towards a TAM-like 'M2-skewed' phenotype with CD206 and pro-inflammatory gene expression including IL-6, TNF and MCP-1, reminiscent of TAMs observed in CCA [7, 17, 19]. Additionally, CCA-patterned macrophages also upregulated the scavenger receptor MARCO, a marker of immunosuppressive TAMs in many tumour types [41]. Data from progressive CCA in rats demonstrated that Fn14 and MCP-1 upregulation is co-regulated early in CCA development. Furthermore, TWEAK overexpression in CCA promoted a dramatic tumour phenotype alteration by inducing expansion of collagen-producing CAFs, which we show to express Fn14 in a significant proportion of patient iCCAs. By driving inflammatory chemokine production, altering macrophage phenotype via crosstalk with CCA epithelia and promoting fibroblastic growth within the CCA microenvironment via a direct action of TWEAK on CAF proliferation, upregulation of TWEAK/Fn14 signalling appears to be an early driver, promoting the development of a niche that supports tumour growth. Our data using genetic knockout or antibody inhibition of TWEAK downstream events

highlight the potential for clinically relevant therapeutic targeting. A humanised antibody against TWEAK, RG7212, is currently being investigated for its efficacy in treating late stage $Fn14^+$ solid tumours in malignancies including colorectal cancer, melanoma and a cohort of three CCA patients, with antibody treatment well-tolerated. Noteworthy, one of the desired actions of antibody treatment is to reduce serum MCP-1 levels [42, 43].

In addition to affecting the CAF and TAM niche compartments, we also report TWEAK-induced secretion of molecules involved in blood vessel development and angiogenesis from CCA cell lines. Macrophages patterned by TWEAK-inducible factors from SNU-1079 cells also upregulated *VEGF-α* mRNA. Significantly, VEGF-A and VEGF-C from CAFs are important mediators of lymphangiogenesis in CCA [44], which is correlated with poor patient outcomes [45]. We also observed some vascular Fn14 expression in rat and human CCA. TWEAK can stimulate endothelial cell proliferation, following Fn14 upregulation in response to VEGF-A and FGF-2 [46]. Given our in vitro proteomic and macrophage patterning results, combined with observation in patient samples, there is future scope to ascertain the role of TWEAK/Fn14 signalling in metastatic progression by acting directly on endothelium, and indirectly via secretion of proteins from tumour cells, tumour-conditioned TAMs and CAFs, which promote tumour progression via pathways such as VEGF-A and VEGF-C.

Our study provides a detailed and novel mechanistic framework of how the TWEAK/Fn14 pathway is involved in building a tumour-permissive niche, acting on TAMs and CAFs in CCA, which both drive chemotherapy resistance [47]. Given the significant proportion of CCA patients exhibiting aberrant upregulation of Fn14, targeting TWEAK/Fn14, may provide

avenues to interrupt epithelial-stromal crosstalk to create novel therapeutics for a cancer where effective treatments are urgently required.

Abbreviations: **AKT-** Protein Kinase B; **CAF-**Cancer-Associated Fibroblast; **CCA-** Cholangiocarcinoma; **CCR2-** C-C Chemokine Receptor type 2; **CK-** Cytokeratin; **CX3CL1-** (C-X3-C motif) Ligand 1;**ERK-** Extracellular Signal-Related Kinase; **Fn14-** Fibroblast Growth Factor-Inducible; **GM-CSF-** Granulocyte Macrophage Colony Stimulating Factor; **HCC-** Hepatocellular Carcinoma; **HMDM-** Human Monocyte-Derived Macrophage; **HPC-** Hepatic Progenitor Cell; **IL-** Interleukin; **MARCO-** Macrophage Receptor with Collagenous Structure; **MCP-1-** Monocyte Chemoattractant Protein 1; **M-CSF-** Macrophage Colony-Stimulating Factor; **MMP-** Matrix Metalloprotease; **NF-** Nuclear Factor; **NICD-** Notch Intracellular Domain; **SDF-** Stromal-Derived Factor; **TAA-** Thioacetamide; **TAM-** Tumour-Associated Macrophage; **TCGA-** The Cancer Genome Atlas; **TIMP-** Tissue Inhibitors of Metalloproteases; **TREM-2-** Triggering Receptor Expressed on Myeloid Cells-2; **TWEAK-** TNF-Like Weak Inducer of Apoptosis; **αSMA-** α-Smooth Muscle Actin

Acknowledgements: The authors acknowledge L. Burkly (Biogen) for providing Fn14 knockout mice. H. McGrath and A. Booth for help with animal experiments, R. Aird and I. Smith for technical assistance and F. Rossi and C. Cryer for flow cytometry assistance.

REFERENCES

[1] Lau SK, Prakash S, Geller SA, Alsabeh R. Comparative immunohistochemical profile of hepatocellular carcinoma, cholangiocarcinoma, and metastatic adenocarcinoma. Hum Pathol 2002;33:1175-1181.

[2] Rullier A, Le Bail B, Fawaz R, Blanc JF, Saric J, Bioulac-Sage P. Cytokeratin 7 and 20 expression in cholangiocarcinomas varies along the biliary tract but still differs from that in colorectal carcinoma metastasis. Am J Surg Pathol 2000;24:870-876.

[3] Banales JM, Marin JJG, Lamarca A, Rodrigues PM, Khan SA, Roberts LR, et al. Cholangiocarcinoma 2020: the next horizon in mechanisms and management. Nat Rev Gastroenterol Hepatol 2020;17:557-588.

[4] Rizvi S, Khan SA, Hallemeier CL, Kelley RK, Gores GJ. Cholangiocarcinoma - evolving concepts and therapeutic strategies. Nat Rev Clin Oncol 2018;15:95-111.

[5] Mavros MN, Economopoulos KP, Alexiou VG, Pawlik TM. Treatment and Prognosis for Patients With Intrahepatic Cholangiocarcinoma: Systematic Review and Meta-analysis. JAMA Surg 2014;149:565-574.

[6] Loilome W, Bungkanjana P, Techasen A, Namwat N, Yongvanit P, Puapairoj A, et al. Activated macrophages promote Wnt/beta-catenin signaling in cholangiocarcinoma cells. Tumour Biol 2014;35:5357-5367.

[7] Boulter L, Guest RV, Kendall TJ, Wilson DH, Wojtacha D, Robson AJ, et al. WNT signaling drives cholangiocarcinoma growth and can be pharmacologically inhibited. J Clin Invest 2015;125:1269-1285.

[8] Sekiya S, Suzuki A. Intrahepatic cholangiocarcinoma can arise from Notch-mediated conversion of hepatocytes. J Clin Invest 2012;122:3914-3918.

[9] Guest RV, Boulter L, Dwyer BJ, Kendall TJ, Man TY, Minnis-Lyons SE, et al. Notch3 drives development and progression of cholangiocarcinoma. Proc Natl Acad Sci U S A 2016;113:12250-12255.

[10] Fingas CD, Bronk SF, Werneburg NW, Mott JL, Guicciardi ME, Cazanave SC, et al. Myofibroblast-derived PDGF-BB promotes Hedgehog survival signaling in cholangiocarcinoma cells. Hepatology 2011;54:2076-2088.

[11] Cadamuro M, Nardo G, Indraccolo S, Dall'olmo L, Sambado L, Moserle L, et al. Platelet-derived growth factor-D and Rho GTPases regulate recruitment of cancer-associated fibroblasts in cholangiocarcinoma. Hepatology 2013;58:1042-1053.

[12] Ohira S, Sasaki M, Harada K, Sato Y, Zen Y, Isse K, et al. Possible regulation of migration of intrahepatic cholangiocarcinoma cells by interaction of CXCR4 expressed in carcinoma cells with tumor necrosis factor-alpha and stromal-derived factor-1 released in stroma. Am J Pathol 2006;168:1155-1168.

[13] Gentilini A, Rombouts K, Galastri S, Caligiuri A, Mingarelli E, Mello T, et al. Role of the stromal-derived factor-1 (SDF-1)-CXCR4 axis in the interaction between hepatic stellate cells and cholangiocarcinoma. J Hepatol 2012;57:813-820.

[14] Okabe H, Beppu T, Ueda M, Hayashi H, Ishiko T, Masuda T, et al. Identification of CXCL5/ENA-78 as a factor involved in the interaction between cholangiocarcinoma cells and cancer-associated fibroblasts. Int J Cancer 2012;131:2234-2241.

[15] Techasen A, Loilome W, Namwat N, Dokduang H, Jongthawin J, Yongvanit P. Cytokines released from activated human macrophages induce epithelial mesenchymal transition markers of cholangiocarcinoma cells. Asian Pac J Cancer Prev 2012;13 Suppl:115-118.

[16] Subimerb C, Pinlaor S, Lulitanond V, Khuntikeo N, Okada S, McGrath MS, et al. Circulating CD14(+) CD16(+) monocyte levels predict tissue invasive character of cholangiocarcinoma. Clin Exp Immunol 2010;161:471-479.

[17] Hasita H, Komohara Y, Okabe H, Masuda T, Ohnishi K, Lei XF, et al. Significance of alternatively activated macrophages in patients with intrahepatic cholangiocarcinoma. Cancer Sci 2010;101:1913-1919.

[18] Raggi C, Correnti M, Sica A, Andersen JB, Cardinale V, Alvaro D, et al. Cholangiocarcinoma stem-like subset shapes tumor-initiating niche by educating associated macrophages. J Hepatol 2017;66:102-115.

[19] Subimerb C, Pinlaor S, Khuntikeo N, Leelayuwat C, Morris A, McGrath MS, et al. Tissue invasive macrophage density is correlated with prognosis in cholangiocarcinoma. Mol Med Rep 2010;3:597-605.

[20] Burkly LC, Michaelson JS, Hahm K, Jakubowski A, Zheng TS. TWEAKing tissue remodeling by a multifunctional cytokine: role of TWEAK/Fn14 pathway in health and disease. Cytokine 2007;40:1-16.

[21] Tirnitz-Parker JE, Viebahn CS, Jakubowski A, Klopcic BR, Olynyk JK, Yeoh GC, et al. Tumor necrosis factor-like weak inducer of apoptosis is a mitogen for liver progenitor cells. Hepatology 2010;52:291-302.

[22] Bird TG, Lu WY, Boulter L, Gordon-Keylock S, Ridgway RA, Williams MJ, et al. Bone marrow injection stimulates hepatic ductular reactions in the absence of injury via macrophage-mediated TWEAK signaling. Proc Natl Acad Sci U S A 2013;110:6542-6547.

[23] Wilhelm A, Shepherd EL, Amatucci A, Munir M, Reynolds G, Humphreys E, et al. Interaction of TWEAK with Fn14 leads to the progression of fibrotic liver disease by directly modulating hepatic stellate cell proliferation. J Pathol 2016;239:109-121.

[24] Ramachandran P, Dobie R, Wilson-Kanamori JR, Dora EF, Henderson BEP, Luu NT, et al. Resolving the fibrotic niche of human liver cirrhosis at single-cell level. Nature 2019.

[25] Kawakita T, Shiraki K, Yamanaka Y, Yamaguchi Y, Saitou Y, Enokimura N, et al. Functional expression of TWEAK in human hepatocellular carcinoma: possible implication in cell proliferation and tumor angiogenesis. Biochem Biophys Res Commun 2004;318:726-733.

[26] Ma L, Hernandez MO, Zhao Y, Mehta M, Tran B, Kelly M, et al. Tumor Cell Biodiversity Drives Microenvironmental Reprogramming in Liver Cancer. Cancer Cell 2019;36:418-430.e416.

[27] Andersen JB, Spee B, Blechacz BR, Avital I, Komuta M, Barbour A, et al. Genomic and genetic characterization of cholangiocarcinoma identifies therapeutic targets for tyrosine kinase inhibitors. Gastroenterology 2012;142:1021-1031.e1015.

[28] Guest RV, Boulter L, Kendall TJ, Minnis-Lyons SE, Walker R, Wigmore SJ, et al. Cell lineage tracing reveals a biliary origin of intrahepatic cholangiocarcinoma. Cancer Res 2014;74:1005-1010.

[29] Elsharkawy AM, Mann DA. Nuclear factor-kappaB and the hepatic inflammation-fibrosis-cancer axis. Hepatology 2007;46:590-597.

[30] Fan B, Malato Y, Calvisi DF, Naqvi S, Razumilava N, Ribback S, et al. Cholangiocarcinomas can originate from hepatocytes in mice. J Clin Invest 2012;122:2911-2915.

[31] Guest RV, Boulter L, Dwyer BJ, Forbes SJ. Understanding liver regeneration to bring new insights to the mechanisms driving cholangiocarcinoma. NPJ Regen Med 2017;2:13.

[32] Jakubowski A, Ambrose C, Parr M, Lincecum JM, Wang MZ, Zheng TS, et al. TWEAK induces liver progenitor cell proliferation. J Clin Invest 2005;115:2330-2340.

[33] Marra F, Tacke F. Roles for chemokines in liver disease. Gastroenterology 2014;147:577-594 e571.

[34] Bettermann K, Vucur M, Haybaeck J, Koppe C, Janssen J, Heymann F, et al. TAK1 suppresses a NEMO-dependent but NF-kappaB-independent pathway to liver cancer. Cancer Cell 2010;17:481-496.

[35] Luedde T, Beraza N, Kotsikoris V, van Loo G, Nenci A, De Vos R, et al. Deletion of NEMO/IKKgamma in liver parenchymal cells causes steatohepatitis and hepatocellular carcinoma. Cancer Cell 2007;11:119-132.

[36] Inokuchi S, Aoyama T, Miura K, Osterreicher CH, Kodama Y, Miyai K, et al. Disruption of TAK1 in hepatocytes causes hepatic injury, inflammation, fibrosis, and carcinogenesis. Proc Natl Acad Sci U S A 2010;107:844-849.

[37] Dambach DM, Watson LM, Gray KR, Durham SK, Laskin DL. Role of CCR2 in macrophage migration into the liver during acetaminophen-induced hepatotoxicity in the mouse. Hepatology 2002;35:1093-1103.

[38] Karlmark KR, Weiskirchen R, Zimmermann HW, Gassler N, Ginhoux F, Weber C, et al. Hepatic recruitment of the inflammatory Gr1+ monocyte subset upon liver injury promotes hepatic fibrosis. Hepatology 2009;50:261-274.

[39] Teng KY, Han J, Zhang X, Hsu SH, He S, Wani NA, et al. Blocking the CCL2-CCR2 Axis Using CCL2-Neutralizing Antibody Is an Effective Therapy for Hepatocellular Cancer in a Mouse Model. Mol Cancer Ther 2017;16:312-322.

[40] Li X, Yao W, Yuan Y, Chen P, Li B, Li J, et al. Targeting of tumour-infiltrating macrophages via CCL2/CCR2 signalling as a therapeutic strategy against hepatocellular carcinoma. Gut 2017;66:157-167.

[41] Lopez-Yrigoyen M, Cassetta L, Pollard JW. Macrophage targeting in cancer. Ann N Y Acad Sci 2020.

[42] Lassen UN, Meulendijks D, Siu LL, Karanikas V, Mau-Sorensen M, Schellens JH, et al. A phase I monotherapy study of RG7212, a first-in-class monoclonal antibody targeting TWEAK signaling in patients with advanced cancers. Clin Cancer Res 2015;21:258-266.

[43] Meulendijks D, Lassen UN, Siu LL, Huitema AD, Karanikas V, Mau-Sorensen M, et al. Exposure and Tumor Fn14 Expression as Determinants of Pharmacodynamics of the Anti-TWEAK Monoclonal Antibody RG7212 in Patients with Fn14-Positive Solid Tumors. Clin Cancer Res 2016;22:858-867.

[44] Cadamuro M, Brivio S, Mertens J, Vismara M, Moncsek A, Milani C, et al. Platelet-derived growth factor-D enables liver myofibroblasts to promote tumor lymphangiogenesis in cholangiocarcinoma. J Hepatol 2019;70:700-709.

[45] Sha M, Jeong S, Wang X, Tong Y, Cao J, Sun HY, et al. Tumor-associated lymphangiogenesis predicts unfavorable prognosis of intrahepatic cholangiocarcinoma. BMC Cancer 2019;19:208.

[46] Harada N, Nakayama M, Nakano H, Fukuchi Y, Yagita H, Okumura K. Pro-inflammatory effect of TWEAK/Fn14 interaction on human umbilical vein endothelial cells. Biochem Biophys Res Commun 2002;299:488-493.

[47] Cadamuro M, Brivio S, Spirli C, Joplin RE, Strazzabosco M, Fabris L. Autocrine and Paracrine Mechanisms Promoting Chemoresistance in Cholangiocarcinoma. Int J Mol Sci 2017;18.

FIGURE LEGENDS

Figure 1. TWEAK/Fn14 expression in cholangiocarcinoma (CCA). (A) Fn14 immunohistochemistry in archival paraffin sections of patient-matched intrahepatic CCA (iCCA) versus non-involved areas of surrounding liver (SL; n=42 iCCA vs. n=26 SL) (B) Quantification of Fn14 immunostaining (Mann-Whitney U test). (C) Single cell RNA-sequencing data of iCCA (GSE125449; n=5 per cohort). Cell types: B-cells, cancer-associated fibroblasts (CAF), hepatic progenitor cells (HPC), malignant cells (Malig.), tumour-associated macrophages (TAM), T-cells, tumour endothelial cells (TEC), undefined. (D) Staining of Fn14 (red) in tumour cells (PanCK; white) and CAFs (αSMA; green) in an iCCA tissue microarray. Nuclei are stained with DAPI (blue). Proportion of $Fn14^{+}$ tumour cells (n=84) and CAFs (n=74) by tumour grade (Kruskal-Wallis test with Dunn's multiple comparison test). Data are mean ± SEM. *p<0.05,**p<0.01. Scale bars represent 100 µm.

Figure 2. TWEAK/Fn14 upregulation in rodent cholangiocarcinoma (CCA). (A) Schematic of thioacetamide (TAA) treatment of rats to induce CCA. (B) Dual immunofluorescence reveals $Fn14^{+}$ (green) tumour epithelia ($PanCK^{+}$; red). (C) mRNA expression of Fn14 and TWEAK in a time course of TAA treatment in rats (n=3 to 11; Kruskal-Wallis with Dunn's post-test) (D) Schematic of TAA treatment of Krt19-CreERTR26-eYFPp53$^{flox/het/wt}$ mice to induce CCA. (E) mRNA expression of Fn14 and TWEAK in Krt19-CreERTR26-eYFPp53$^{Fl/WT}$ or Krt19-CreERTR26-eYFPp53$^{WT/WT}$ ($p53^{wt/het}$; no CCA, n=9) vs. Krt19-CreERTR26-eYFPp53$^{flox/flox}$ ($p53^{f/f}$; CCA, n=6; Mann-Whitney U test). (F) Protein expression of Fn14 in mouse $p53^{wt/het}$ vs. $p53^{flox/flox}$ mice (n=7 each; unpaired t-test). Data are mean ± SEM. *p<0.05,**p<0.01.***p<0.001. Scale bars represent 50 µm.

Figure 3. TWEAK signalling drives NF-κB pathway activation and protein production. (A) TWEAK-dependent modulation of NF-κB pathway proteins in cholangiocarcinoma (CCA) cells and quantification of NF-κB protein expression 2h-post rhTWEAK exposure. (B) Localisation of NF-κB p65 subunit in CCA cell lines with TWEAK treatment. (C) MTT assay in CCA lines following 72 h treatment with increasing dose of rhTWEAK. (D) TWEAK-dependent mRNA expression in CCA lines following 6 h rhTWEAK treatment. (E) Protein immunoassay of secreted proteins from CCA lines treated with PBS or rhTWEAK. Data are mean ± SEM. unpaired t-test (n=3) or one-way ANOVA with Dunnett's post-test (MTT assay; n=6); *p<0.05,**p<0.01,***p<0.001. Scale bars represent 50 μm.

Figure 4. Cholangiocarcinoma (CCA)-derived TWEAK-inducible factors drive macrophage patterning. (A) Cell surface CD206 expression (median fluorescence intensity; MFI) in HMDMs treated with conditioned medium (CM) from PBS- or TWEAK-treated CCA cells (One-way ANOVA with Tukey's post-test; n=3). (B) mRNA expression in HMDMs treated with conditioned medium from PBS- or TWEAK-treated CCA cells (n=3). Fold changes expression was calculated compared to control DMEM with PBS (DMEM+PBS) and analysed using one-way ANOVA with Dunnett's multiple comparison test. *p<0.05,**p<0.01,***p<0.001. Data are mean ± SEM.

Figure 5. MCP-1 expression in cholangiocarcinoma (CCA). (A) MCP-1 immunohistochemistry in archival paraffin sections of patient-matched intrahepatic CCA (iCCA) versus adjacent non-involved surrounding liver areas (SL). (B) Digital pixel analysis of sections (n=42 iCCA vs. n=26 SL; Mann-Whitney U test). (C) Staining of tumour liver tissue from an iCCA tissue microarray (n=89) with PanCK (white), Fn14 (red), MCP-1 (green). Nuclei are stained with DAPI (blue). (D) Analysis of total distribution of MCP-1^+ cells in $Fn14^-$ and $Fn14^+$ subsets of $PanCK^+$ tumour cells in individual CCA tissues or stratified with respect to tumour grade (Wilcoxon matched-pairs signed rank test). (E) Assessment of distribution in MCP-1^+ cells (red) in $CD68^+$ macrophages (green) and αSMA^+ CAFs (white). Nuclei are stained with DAPI (blue). Data are mean ± SEM. *p<0.05,**p<0.01,****p<0.0001. Scale bars represent 100 μm.

Figure 6. MCP-1 in rodent cholangiocarcinoma (CCA). (A) MCP-1 immunohistochemistry (IHC) in liver from rats administered TAA for 10 weeks (injured, pre-malignant) up to 26 weeks. (B) Triple immunofluorescence reveals MCP-1^+ tumour epithelia ($PanCK^+$) with interspersed macrophage infiltration (CD68) in rat CCA. (C) mRNA expression of MCP-1 in a time course of TAA treatment in rats (n=3-11 per timepoint; Kruskal-Wallis test with Dunn's post-test). (D) Triple immunofluorescence reveals MCP-1^+ tumour epithelia ($PanCK^+$) with interspersed macrophage infiltration ($F4/80^+$) in Krt19-CreERTR26-eYFPp$53^{Fl/Fl}$ mice administered TAA for 26 weeks to induce CCA. (E) Schematic of xenograft experiments. (F) SNU-1079 xenografts in CD-1 nude mice treated with control or anti-MCP-1 antibody (n=8 per group; unpaired t-test). (G) Macrophage marker (F4/80, CD206) staining of SNU-1079 xenografts (n=7 isotype vs. n=6 treated with anti-MCP-1; Mann-Whitney U test). (H) Analysis of peripheral blood monocytes of xenografted CD-1 nude mice (n=7 isotype vs. n=8 anti-MCP-

1 treated; unpaired t-test). Data are mean ± SEM. *p<0.05,**p<0.01,***p<0.001. Scale bars represent 50 μm.

Figure 7. TWEAK drives cancer-associated fibroblast (CAF) proliferation in cholangiocarcinoma (CCA). CCA was induced in mice with overexpression of Notch Intra-Cellular Domain and AKT (NICD/AKT) with effects of TWEAK overexpression (NICD/AKT+TWEAK) assessed. (A) Gross morphology of livers. (B) Haematoxylin and eosin-stained liver sections. (C) Tumour area (Mann-Whitney U test) and cystic and tumour epithelial area quantification. (D) Staining of biliary tissue (CK19) and phosphorylated NF-kB p65 (p-p65) in normal and CCA areas. (E) Staining of biliary tissue and proliferation marker (Ki67). (F) Quantification of CAF (αSMA^+) area and collagen deposition (Picrosirius Red (PSR) staining). (G) Staining of CAF (αSMA) and p-p65 or proliferation marker (Ki67). Data are mean ± SEM. *p<0.05,***p<0.001,****p<0.0001. Unpaired t-test unless otherwise stated. Scale bars represent 100 μm.

Figure 1.

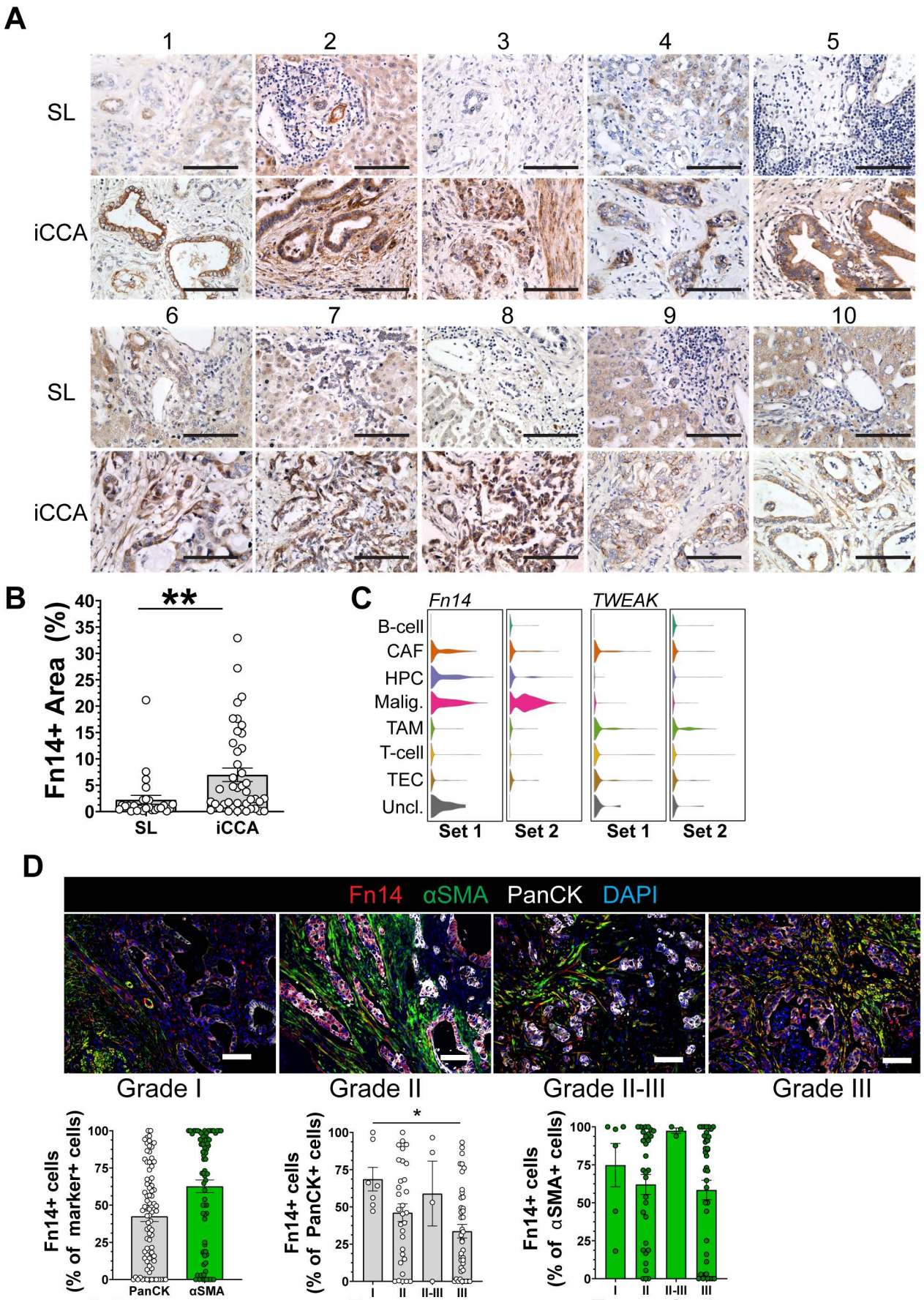
A
1
2
3
4
5
SL
iCCA
6
7
8
9
10
SL
iCCA
B
**
Fn14+ Area (%)
40
35
30
25
20
15
10
5
0
SL
iCCA
C
Fn14
TWEAK
B-cell
CAF
HPC
Malig.
TAM
T-cell
TEC
Uncl.
Set 1
Set 2
Set 1
Set 2
D
Fn14 αSMA PanCK DAPI
Grade I
Grade II
Grade II-III
Grade III
Fn14+ cells (% of marker+ cells)
100
75
50
25
0
PanCK
αSMA
Cellular compartment
Fn14+ cells (% of PanCK+ cells)
*
I
II
II-III
III
Tumour Grade
Fn14+ cells (% of αSMA+ cells)
I
II
II-III
III
Tumour Grade

Figure 2.

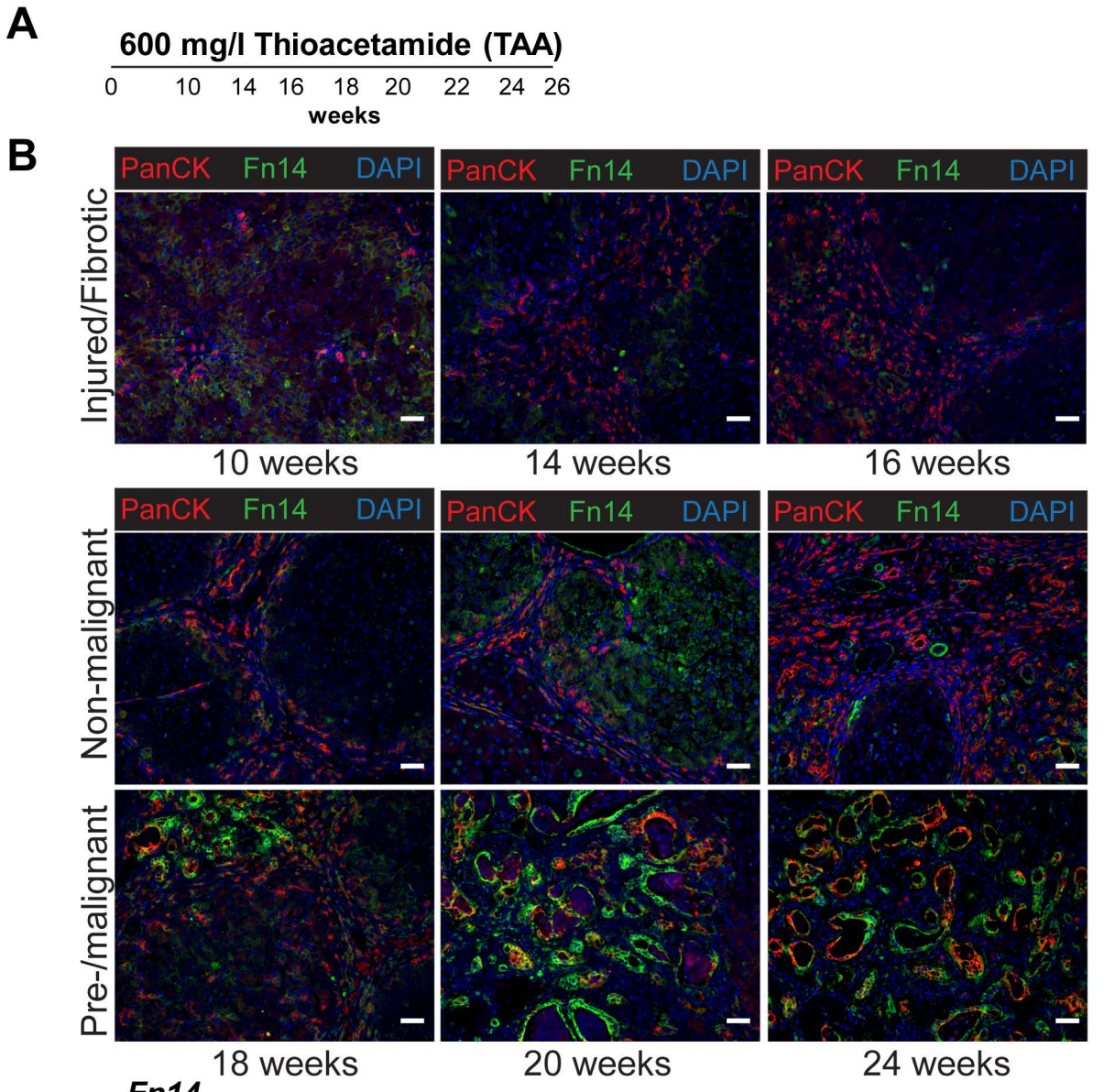
A
600 mg/l Thioacetamide (TAA)
0 10 14 16 18 20 22 24 26
weeks
B
PanCK Fn14 DAPI
Injured/Fibrotic
10 weeks
14 weeks
16 weeks
Non-malignant
Pre-/malignant
18 weeks
20 weeks
24 weeks

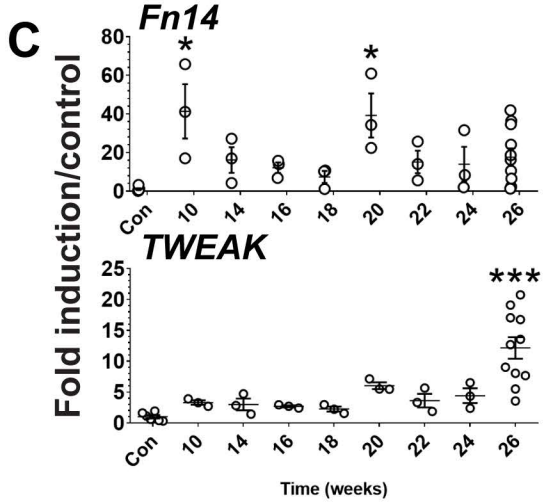
C
Fn14
TWEAK
Fold induction/control
Con 10 14 16 18 20 22 24 26
Time (weeks)

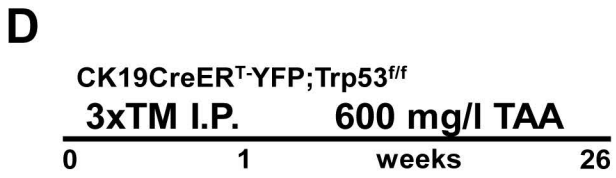
D
CK19CreER^T-YFP;Trp53^f/f
3xTM I.P.
600 mg/l TAA
0 1 weeks 26

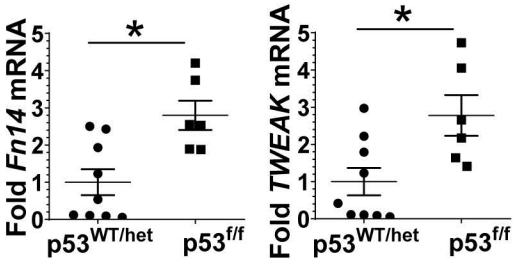
E
Fold Fn14 mRNA
Fold TWEAK mRNA
p53WT/het
p53f/f

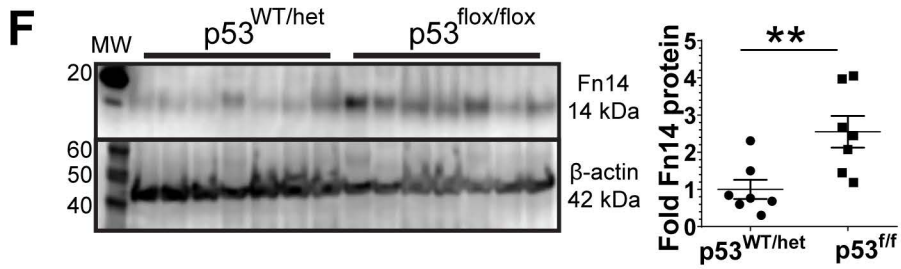
F
MW
p53WT/het
p53flox/flox
20
60
50
40
Fn14
14 kDa
β-actin
42 kDa
Fold Fn14 protein
p53WT/het
p53f/f

Figure 3.

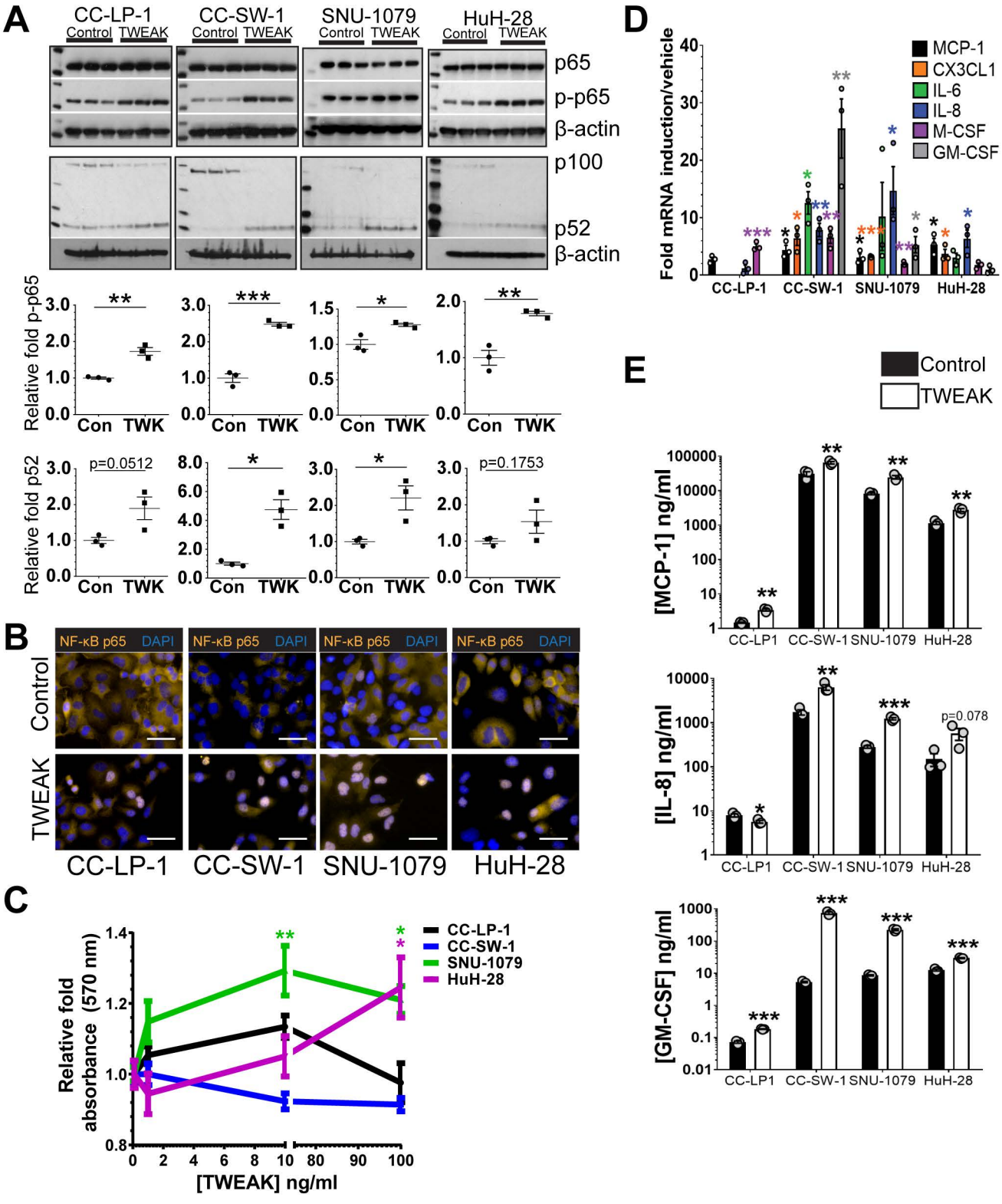
A
CC-LP-1
CC-SW-1
SNU-1079
HuH-28
Control TWEAK
p65
p-p65
β-actin
p100
p52
β-actin
Relative fold p-p65
Relative fold p52
Con TWK
p=0.0512
p=0.1753
B
NF-κB p65 DAPI
Control
TWEAK
CC-LP-1 CC-SW-1 SNU-1079 HuH-28
C
Relative fold absorbance (570 nm)
[TWEAK] ng/ml
CC-LP-1
CC-SW-1
SNU-1079
HuH-28
D
Fold mRNA induction/vehicle
MCP-1
CX3CL1
IL-6
IL-8
M-CSF
GM-CSF
CC-LP-1 CC-SW-1 SNU-1079 HuH-28
E
Control
TWEAK
[MCP-1] ng/ml
[IL-8] ng/ml
[GM-CSF] ng/ml
CC-LP1 CC-SW-1 SNU-1079 HuH-28
p=0.078

Figure 4.

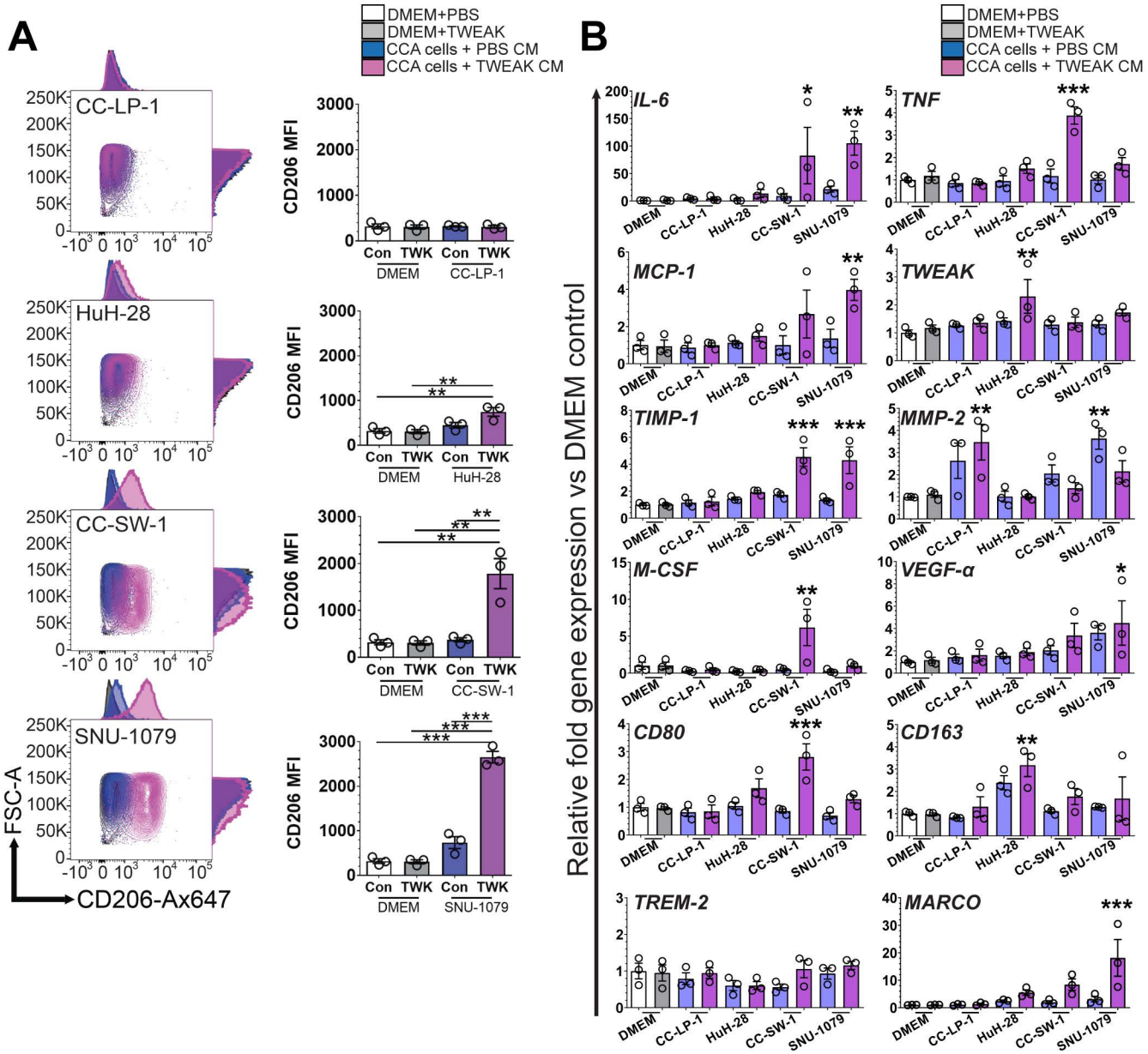
A
DMEM+PBS
DMEM+TWEAK
CCA cells + PBS CM
CCA cells + TWEAK CM
CC-LP-1
HuH-28
CC-SW-1
SNU-1079
FSC-A
CD206-Ax647
CD206 MFI
Con TWK Con TWK
DMEM
CC-LP-1
HuH-28
CC-SW-1
SNU-1079
B
Relative fold gene expression vs DMEM control
IL-6
TNF
MCP-1
TWEAK
TIMP-1
MMP-2
M-CSF
VEGF-α
CD80
CD163
TREM-2
MARCO
DMEM
CC-LP-1
HuH-28
CC-SW-1
SNU-1079

Figure 5.

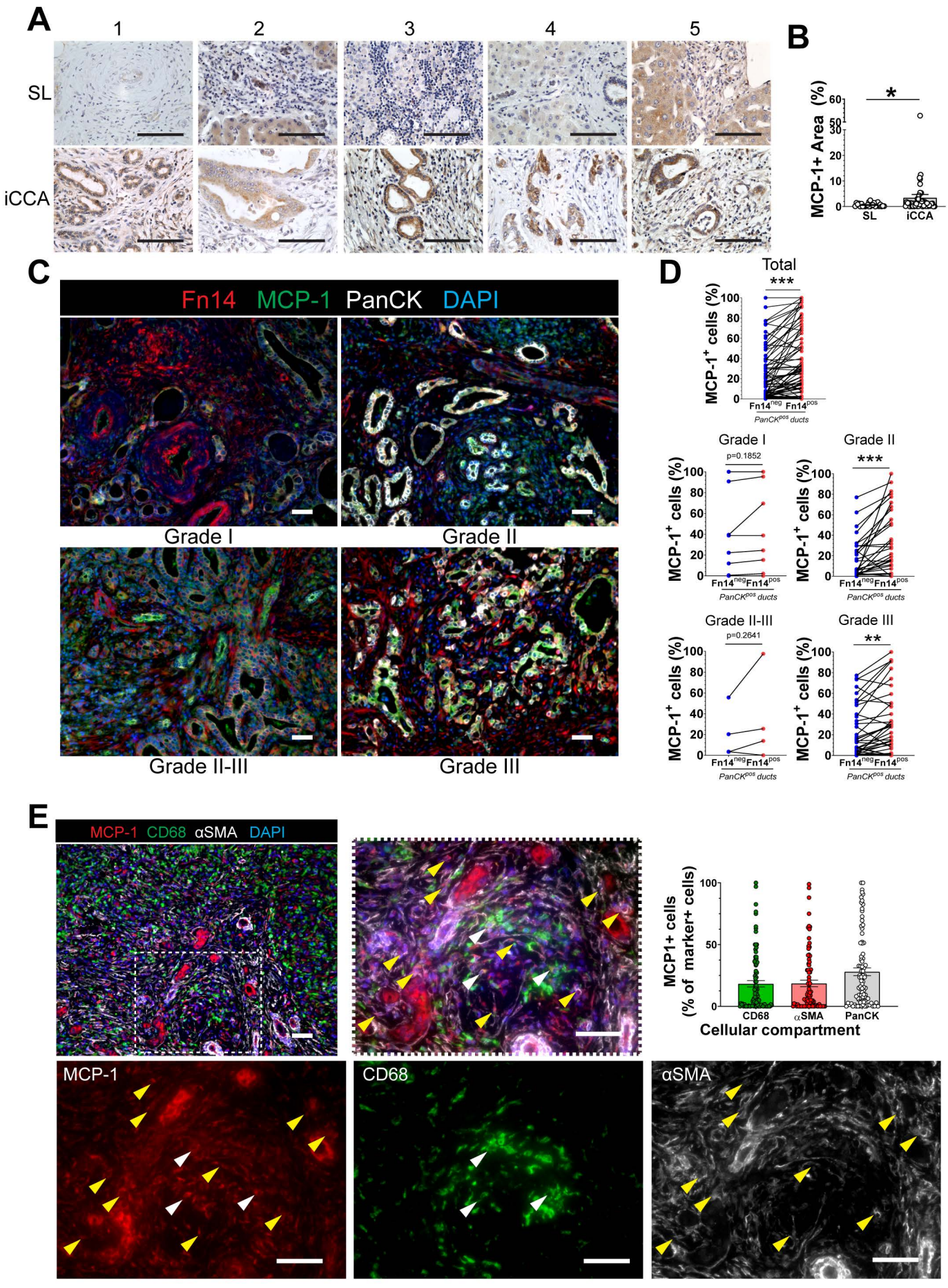
A
1
2
3
4
5
SL
iCCA
B
MCP-1+ Area (%)
SL
iCCA
C
Fn14 MCP-1 PanCK DAPI
Grade I
Grade II
Grade II-III
Grade III
D
Total
MCP-1+ cells (%)
Fn14neg Fn14pos
PanCKpos ducts
Grade I
p=0.1852
Grade II
Grade II-III
p=0.2641
Grade III
E
MCP-1 CD68 αSMA DAPI
MCP1+ cells (% of marker+ cells)
CD68
αSMA
PanCK
Cellular compartment
MCP-1
CD68
αSMA

Figure 6.

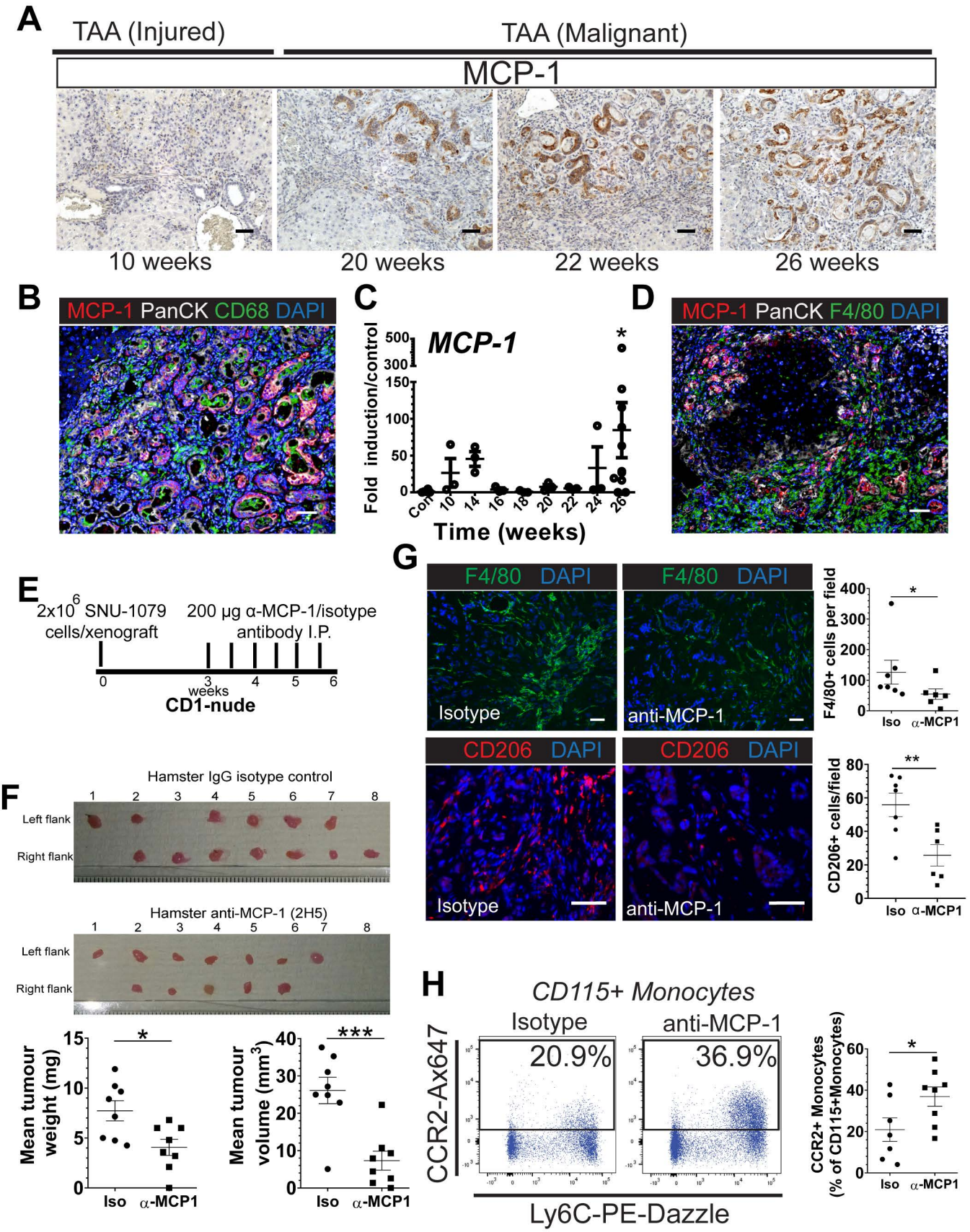
A
TAA (Injured)
TAA (Malignant)
MCP-1
10 weeks
20 weeks
22 weeks
26 weeks
B
MCP-1 PanCK CD68 DAPI
C
MCP-1
Fold induction/control
Time (weeks)
D
MCP-1 PanCK F4/80 DAPI
E
2x10^6 SNU-1079 cells/xenograft
200 µg α-MCP-1/isotype antibody I.P.
weeks
CD1-nude
F
Hamster IgG isotype control
Left flank
Right flank
Hamster anti-MCP-1 (2H5)
Mean tumour weight (mg)
Mean tumour volume (mm3)
Iso
α-MCP1
G
F4/80 DAPI
Isotype
anti-MCP-1
F4/80+ cells per field
CD206 DAPI
CD206+ cells/field
H
CD115+ Monocytes
CCR2-Ax647
Ly6C-PE-Dazzle
20.9%
36.9%
CCR2+ Monocytes (% of CD115+Monocytes)

Figure 7.

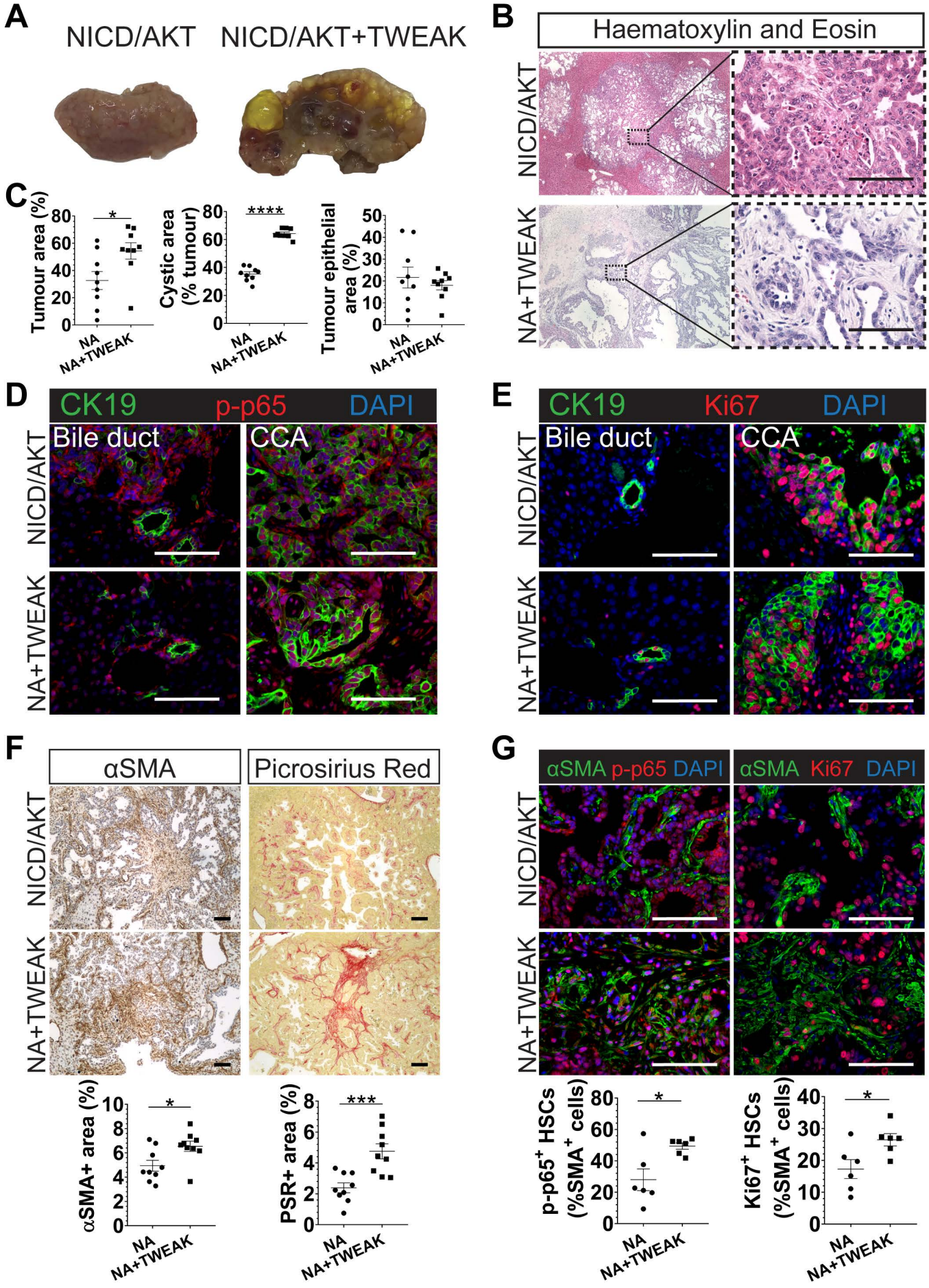
A
NICD/AKT
NICD/AKT+TWEAK
B
Haematoxylin and Eosin
NICD/AKT
NA+TWEAK
C
Tumour area (%)
Cystic area (% tumour)
Tumour epithelial area (%)
NA
NA+TWEAK
D
CK19
p-p65
DAPI
Bile duct
CCA
E
CK19
Ki67
DAPI
F
αSMA
Picrosirius Red
αSMA+ area (%)
PSR+ area (%)
G
αSMA p-p65 DAPI
αSMA Ki67 DAPI
p-p65+ HSCs (%SMA+ cells)
Ki67+ HSCs (%SMA+ cells)

Highlights:

1. Fn14 is upregulated in on tumour cells and cancer associated fibroblasts, and TWEAK is expressed by tumour associated macrophages in human CCA. TWEAK/Fn14 are progressively upregulated during rodent tumour development, with Fn14 upregulated in dysplastic biliary lesions in pre-neoplastic liver in rats.
2. TWEAK/Fn14 signalling induces tumour associated macrophage accumulation via TWEAK-inducible MCP-1 chemotaxis which can be blocked in vivo.
3. TWEAK-inducible factors from tumour cells pattern macrophages to a TAM-like phenotype, upregulating CD206, and the expression of MCP-1, IL-6, TNF, VEGF-α and MARCO
4. TWEAK overexpression in experimental tumour formation drives CAF proliferation, collagen deposition and increases macrophages in mice, whilst tumour formation is reduced with genetic deletion of Fn14.

ICMJE disclosure form